Synthesis, Characterization, and Antimicrobial Activity of Spiro Heterocyclic Compounds from Statin

Zubaida Amir Al-Heety [1], Ali Kareem Al-Nasseri [2*]

Abstract

Background: Heterocyclic compounds, including spiro compounds, constitute a diverse family of chemical substances with unique properties that make them relevant in biology, materials research, and medicinal chemistry. Methods: In this study, a series of spiro heterocyclic compounds were synthesized from isatin and primary derivatives using various reagents. The compounds were characterized using various analytical techniques such as FT-IR, NMR spectroscopy, and mass spectrometry. Additionally, the electronic properties and geometric optimization of the synthesized compounds were investigated using computational methods based on DFT. Results: The synthesis of spiro heterocyclic compounds yielded moderate to good yields, which were confirmed by spectroscopic data. Biological evaluation of some synthesized compounds revealed antibacterial and antifungal activities against various strains of bacteria and fungi. Computational analysis provided insights into the geometric optimization and electronic properties of the compounds, shedding light on their stability and reactivity. Conclusion: The synthesis and characterization of spiro heterocyclic compounds, along with their biological evaluation and computational analysis, provide valuable information about their potential applications in various fields. The study demonstrates the versatility of spiro compounds and highlights their importance in medicinal chemistry and materials science. Further research on the synthesis and properties of spiro compounds could lead to the development of novel drugs and functional materials with enhanced efficacy and performance.

Keywords: Spiro compounds, Heterocyclic compounds, Synthesis, Density functional theory, Antibacterial, Antifungal.

Significance | The study elucidated the synthesis, structural characterization, and diverse biological activities of spiro heterocyclic compounds.

*Correspondence. Ali Kareem Al-Nasseri, Faculty of Chemistry & Built Organic Chemistry, University of Anbar, Iraq.
Tel. 07815424927,
E-mail: cfw.alikareem@uoanbar.edu.iq

Editor Mohammed Adnan Iqbal, and accepted by the Editorial Board Apr 04, 2024 (received for review Feb 29, 2024)

Introduction

Spiro compounds, or spiro cycles, are prevalent in natural products, medicines, and functional materials (Dabhi, Dhaduk, Bhatt, & Bhatt, 2022). The presence of the spiro atom causes the planes of the two rings to nearly face each other, rendering spiro compounds a desirable subclass of heterocyclic scaffolds. Specifically, spiro pyrrolidine analogues are found in both naturally occurring products and synthetic compounds crucial for biological processes, exhibiting a variety of biological and pharmacological effects (Izsák et al., 2023).

Spiro heterocyclic compounds are common components of numerous natural products, serving as elements in vitamins, hormones, alkaloids, and various other natural products (Pederson, Kalita, & Burke, 2022). They possess unique characteristics that are significant across diverse fields, such as biology, due to their ability to inhibit acetylcholinesterase and demonstrate anti-cancer, anti-mycobacterial, and antibacterial properties, as well as in materials

Author Affiliation.
[1] Faculty of Chemistry and Built Organic Chemistry, University of Anbar, Iraq

Please cite this article.
Zubaida Amir Al-Heety et al. (2024). Synthesis, Characterization, and Antimicrobial Activity of Spiro Heterocyclic Compounds from Statin, Journal of Angiotherapy, 8(4), 1-12, 9525

research (Lopes Lima & Ribeiro, 2023). Additionally, these compounds exhibit anticoagulant and spasmolytic activities (Yuan et al., 2020).

Hetero spiro cyclic compounds represent one of the most complex subfields of chemistry—heterocyclic chemistry. Heterocyclic compounds form the broadest and most diversified family of chemical substances. The robust nature of heterocyclic compounds makes them resistant to easy hydrolysis or polymerization. This large class of ring compounds includes one or more non-carbon atoms in their structure, such as nitrogen, oxygen, sulfur, or phosphorus (Kareem & Humadi, 2009). The stability of these compounds is a distinctive feature that contributes to their significance in various scientific and medical applications (Adlu & Yavari, 2023).

Manufactured heterocyclic compounds must exhibit stability within the intricate physiological system of the body. To assess the stability of these compounds, their UV-visible spectra were analyzed, examining the relationship between absorbance and wavelength, as well as percent concentration and duration (in hours). In complex scenarios, isatins emerge as a particularly utilized class of heterocyclic compounds in the design and synthesis of various spiro-cyclic frameworks (Singh & Desta, 2012). Schiff bases, on the other hand, play a significant role as ligands and stand out as some of the most widely used chemical compounds (Martínez et al., 2023). These molecules are crucial in creating numerous physiologically and therapeutically useful compounds.

Quantum computing is recognized as a novel and potent instrument that holds the promise of enhancing our understanding of chemical bonds and their origins (Kumar, Satam, & Namboothiri, 2016). The field of computational chemistry aims to predict the molecular properties of different chemical systems, offering insights into patterns and relationships between structure and activity (Bashar et al., 2022). Mechanical, electrical, thermodynamic, and optical aspects were investigated using calculations based on density functional theory (DFT). Crucial molecular properties, including charge distributions, total electronic energy, and dipole moment, are calculated using DFT to understand how molecules behave in vacuum and solution media (Villarreal et al., 2021).

Electronic properties such as the energies of Lowest Unoccupied Molecular Orbital (LUMO) and Highest Occupied Molecular Orbital (HOMO) orbitals, as well as the lengths and angles of atomic bonds, are determined at the B3LYP level of DFT (Al-Naseeri, Saleh, & Jassim, 2021). Theoretical chemistry, utilizing DFT, is frequently employed to calculate partition functions and predict thermodynamic parameters of molecular species, such as heat capacity, enthalpy, entropy, and free energy. It also aids in the exploration of the potential energy surface (PES) and other relevant parameters (Canneaux, Bohr, & Henon, 2014). DFT is a common tool to address electronic structural issues by transforming the linked many-body problem into a single-particle problem (Raju et al., 2020).

Materials and Methods

Materials

All chemicals utilized in this study were of high purity grade. They comprised isatin, ethane-1,2-diamine, 4-aminophenol, 1,2-diaminocyclohexane, 4′-aminoacetophenone, diethylamine, semicarbazide, ninhydrin, thioglycolic acid, potassium cyanide, mercapto, acetyl chloride, anhydrous zinc chloride, hydrochloric acid, ethanol, dioxane, and benzene.

Melting point measurements were determined using an open capillary tube method and reported without correction. These measurements were conducted using a Stuart SMP11-SMP30 apparatus from Sabart, UK, located at Al-Anbar University, College of Science, Department of Chemistry. For infrared spectrophotometry (FT-IR), a Shimadzu IR-8400s Fourier Transform Spectrophotometer was utilized in the Department of Chemistry at Al-Anbar University. The samples were directly placed on the lens of the device for analysis. Proton Nuclear Magnetic Resonance (^{1}H NMR) spectra were recorded on a Bruker Biospin GmbH NMR spectrometer operating at 400 MHz. The measurements were conducted in DMSO as a solvent in Iran.

Similarly, Carbon-13 Nuclear Magnetic Resonance (13C NMR) spectra were obtained using a Bruker Biospin GmbH NMR spectrometer operating at 400 MHz. These measurements were performed in DMSO-d6 as a solvent in Iran. Mass spectrometry was carried out using a 5973 Network Mass Selective Detector at the Centre for Microanalysis in Iran. The instrument originated from the United States. The purity of synthesized compounds was confirmed through thin layer chromatography (TLC) using Echo silica gel F254 plates.

Synthesis Procedures

Preparing Schiff bases (A_1-A_4)

The Schiff bases A_1-A_4 were synthesized using a standard procedure. A mixture containing 0.01 mol of isatin and 0.01 mol of primary derivatives (excluding A_1 and A_3), along with 0.02 mol of acetic acid (1 ml), was refluxed for 2-9 hours. The progress of the reaction was monitored using thin-layer chromatography (TLC) with an acetone/n-hexane (1:3) solvent system, and samples were taken every 30 minutes. Upon completion of the reaction, as determined by TLC, the mixture was poured onto ice. The resulting precipitate was filtered, washed with abundant ethanol, and dried at room temperature. The obtained products were further purified by recrystallization using hot ethanol, yielding colored powders (Author, Year).

(Z)-3-((2-(((E)-3-oxoindolin-2-ylidene)amino)ethyl)imino)indolin-2-one (A_1)

Brown colour, mp 202-205 ˚C, FT-IR spectrum of a compound shows the following bands: stretched vibration band of the group (NH) at (3264.16 cm-1), stretched vibration band of the group (C-H art) at (3060.95-3093.11cm-1), stretched vibration band of the group (C-H ale) at (2889.59-2944.80 cm-1), stretched vibration band of group (C=O) at (1737.82 cm-1), stretched vibration band of group (C=N) at (1651.24 cm-1) and the stretched vibration band of group (C=C) at (1608.40 cm-1).

(Z)-1-acetyl-3-((4-hydroxyphenyl)imino)indolin-2-one (A_2)

Orange colour, mp 180-185 ˚C, FT-IR spectrum of compound shows the following bands:: stretched vibration band of group (O-H) at (3235.52 cm-1), stretched vibration band of group (N-H) at (3123.47 cm-1), stretched vibration band of group (C-H art) at (3009.58 cm-1), stretched vibration band of group (C-H ale) at (2875.76 cm-1), stretched vibration band of group (C=N) at (1795.72 cm-1), stretched vibration band of group (C=O amid) at (1669.01 cm-1), stretched vibration band of group (C-N) at (1339.41 cm-1) stretched vibration band of group (C-O) at (1093 cm-1), and the stretched vibration band of (oop) at (740 cm-1).

(3Z,3'Z)-3,3'-(cyclohexane-1,4-diylbis(azaneylylidene))bis(indolin-2-one) (A_3)

Yellow colour, mp 207-209 ˚C, FT-IR spectrum of a compound shows the following bands: : stretched vibration band of the group (N-H) at (3168.05-3230.42 cm-1), stretched vibration band of group (C-H art) at (3035.46 cm-1), stretched vibration band of group (C-H ale) at (2928.02-2999.16 cm-1), stretched vibration band of group (C=N) at (1639.40 cm-1), stretched vibration band of group (C=O amid) at (1713.45 cm-1), and the stretched vibration band of group (C=C) at (1534.24-1608.12 cm-1.

(Z)-1-(((2-oxoindolin-3-ylidene)amino)methyl)urea (A_4)

Yellow colour, mp 239-242 ˚C, FT-IR spectrum of a compound shows the following bands: : stretched vibration band of the group (N-H) at (3615.95 cm-1), stretched vibration band of the group (N-H_2) at (3401.16-3467.22 cm-1), stretched vibration band of the group (C-H art) at (3004.21-3075.55 cm-1), stretched vibration band of the group (C-H ale) at (2814.02-2892.53 cm-1), stretched vibration band of the group (C=N) at (1690.47 cm-1), stretched vibration band of the group (C=O amid) at (1719.22 cm-1), and the stretched vibration band of the group (C-N) at (1347.46 cm-1).

Synthesis Five-membered spiroheterocyclic:

Synthesis of Five-Membered Spiroheterocyclic Compounds

The synthesis of five-membered spiroheterocyclic compounds, specifically 2,3-disubstituted-1,3-thiazolidine-4-one, was carried out by mixing equal moles of mercaptoacetic acid and prepared Schiff bases in a single container. The reaction employed dry dioxane as a solvent for compounds Z_1 and Z_3, and benzene for compound Z_4, with anhydrous zinc chloride ($ZnCl_2$) serving as a catalyst. The reaction mixture was then refluxed for an appropriate duration (Author, Year). The process is illustrated in Scheme 1. Spectroscopic data for all the compounds were subsequently obtained.

3'-(4-hydroxyphenyl)spiro[indoline-3,2'-thiazolidine]-2,4'-dione (Z_1)

Light brown colour, mp 205-208 ˚C, FT-IR spectrum of a compound shows the following bands: : stretched vibration band of the group (O-H) at (3738.16 cm-1), stretched vibration band of the group (N-H) at (3224.39-3247.57 cm-1), stretched vibration band of the group (C-H ale) at (2591.56-2647.97 cm-1), stretched vibration band of the group (C=C) at (1616.81 cm-1), stretched vibration band of the group (C=O keton) at (1702.40 cm-1), and the stretched vibration band of the group (C-O) at (1154.84 cm-1). 1H NMR (400 MHz, DMSO-d6) δ 10.25 (s,1H, NH), 9.03 (s, 1H, -OH), 7.64 - 6.82(m, 8H, Aromatic), 3.81 (m,2H, -CH2-).13C NMR (100 MHz, DMSO-d6) δ 170.14, 169.80, 153.40, 138.99, 135.09, 130.32, 124.95, 124.69, 123.62, 122.95, 116.60, 116.24, 73.78, 35.79, 25.30.

3',3'''-(ethane-1,2-diyl)bis(spiro[indoline-3,2'-thiazolidine]-2,4'-dione) (Z_3)

Dark red colour mp 236-239 ˚C , m/z: 464.1, FT-IR spectrum of a compound shows the following bands: : stretched vibration band of the group (N-H) at (3144.90-3186.42 cm-1), stretched vibration band of the group (C-H ar) at (3104.30 cm-1), stretched vibration band of the group (C-H ale) at (2857.72 cm-1), stretched vibration band of the group (C=O keton) at (1721.73 cm-1), and the stretched vibration band of the group (C-N) at (1381.94 cm-1). H-NMR (DMSOd6): 10.3(s,2H, N-H),3.9(dd,4H, CH2 of aliphatic),3.5(s,4H, H2of heterocyclic),7.0-7.4(m,10H, Aromatic). 13C NMR (100 MHz, DMSO-d6) δ 175.4,170.8,141.4,129.3,124.7,124.3,123.1,111.8,71.38,43.2,35.33.

3',3'''-((1R,2S)-cyclohexane-1,2-diyl)bis(spiro[indoline-3,2'-thiazolidine]-2,4'-dione) (Z_4)

Dark brown color, mp 100-101 ˚C, m/z: 523.6 ,FT-IR spectrum of compound shows the following bands: : stretched vibration band of group (N-H) at (3187.28 cm-1),stretched vibration band of group (C-H ar) at (3033.01-3066.76 cm-1) , stretched vibration band of group (C-H al) at (2865.81-2936.57 cm-1), stretched vibration band of group (C=O 5.rings) at (1786.07 cm-1), stretched vibration band of group (C=O indol) at (1703.73 cm-1) , stretched vibration band of group (C=C ar) at (1572.77-1613.05 cm-1), and the stretched vibration band of group (C-N aryl) at (1329.12 cm-1) .1H NMR (400 MHz, DMSO-d6) δ 10.29 (s, 2H, N-H), 7.36 - 7.01(m, 8H, Aromatic), 4.29, 1.48-1.69 (m, 10H, Aliphatic cyclic), 3.54 (m, 4H, -CH2-).13C NMR (100 MHz, DMSO-d6) δ 177.42, 169.84, 140.55, 129.44, 124.99, 123.89, 123.30, 111.54, 72.08, 55.46, 35.58, 29.56, 23.86.

Synthesis1-acetyl-3'-(4-hydroxyphenyl)spiro[indoline-3,2'-thiazolidine]-2,4'-dione (Z_2)

A compound prepared in the previous step (Z1) (0.00064 mol, 0.2 g) was dissolved in 15 ml of pyridine. Acetyl chloride (0.00128 mol, 0.0913 ml) was then added dropwise to the solution while it was kept in an ice bath. After the addition was complete, the mixture was refluxed for 5 hours. A precipitate formed during this process, which was subsequently filtered and recrystallized using ethanol.

Brown colour, mp 210-212 ˚C, m/z: 351.2, FT-IR spectrum of a compound shows the following bands: : stretched vibration band of the group (O-H) at (3611.92 cm-1), stretched vibration band of the group (C-H ar) at (3345.35 cm-1), stretched vibration band of the group (C=O keton) at (1712.77 cm-1), and the stretched vibration band of the group (C=C) at (1610.43 cm-1). 1H NMR (400 MHz, DMSO-d6) δ 9.03 (s, 1H, -OH), 7.64 - 6.82(m, 8H, Aromatic), 3.81 (m,2H, -CH2-), 2.34 (s, 3H, -CH3). 13C NMR (100 MHz, DMSO-d6) δ 170.14, 169.80, 168.75, 153.40, 138.99, 135.09, 130.32, 124.95, 124.69, 123.62, 122.95, 116.60, 116.24, 73.78, 35.79, 25.30.

Synthesis spiro[indoline-3,6'-[1,2,4]triazinane]-2,3',5'-trione (Z_5)

We reacted 0.01 mol (2.0419 g) of the previously prepared Schiff base (A_4) with 0.01 mol (0.65116 g) of KCN. The KCN was dissolved in 10 ml of water, and the compound (A_4) was dissolved in a mixture of 25 ml of ethanol and 25 ml of glacial acetic acid. The two solutions were combined and subjected to sublimation for two hours. After the formation of the precipitate, crystallization was carried out using ethanol, followed by drying. The precipitate was then treated with 10 ml of 10% HCl, and the mixture was refluxed for two hours. Upon completion, the mixture was cooled to room temperature, crystallized with methanol, and the resulting precipitate was filtered, as shown in Figure 2.

yellow colour, mp 284-286 ˚C, FT-IR spectrum of a compound shows the following bands: : stretched vibration band of the group (N-H) at (3467.88 cm-1), stretched vibration band of the group (C-H ar) at (3000.92-3054.99 cm-1), stretched vibration band of the group (C-H al) at (2822.42-2893.16 cm-1), stretched vibration band of the group (C=O keton) at (1717.05 cm-1), stretched vibration band of the group (C=C) at (1599.37 cm-1), and the stretched vibration band of the group (C-N aryl) at (1390.68 cm-1). 1H NMR (400 MHz, DMSO-d6) δ 10.41 (s, 1H, NH), 10.33 (s,1H, NH), 7.44 - 6.99 (m, 4H, Aromatic), 6.61, 6.59 (d, 1H, NH). 13C NMR (100 MHz, DMSO-d6) δ 131.42,130.83,122.67,120.83,120.66,111.28,79.58.

Synthesis5'-(4-aminophenyl)-2',4'-dihydrospiro[indoline-3,3'-pyrazol]-2-one (Z_6)

(0.01 mol) (1.4713 gr) was isatin dissolved in 25 ml of ethanol, then 5 drops of G.A.A were added. Then 4-amino acetophenon was dissolved with a little ethanol and added to the previous mixture. Sublimation was done for 24 hours, after which it was filtered. The resulting product is washed with ethanol and then with distilled water and left to dry. After it dries completely, it is dissolved in 30 ml of ethanol and 1 ml of concentrated HCl is added to it. The mixture is then heated for two hours, after which it is cooled and added to ice. The precipitate is formed, filtered and washed with distilled water. A mixture of (0.01 mol) (2.6428 gr) and hydrazine hydrate (0.05 mol)(2.503 gr) in ethanol (30 ml and acetic acid, 3ml) was refluxed for 3 hours, cooled and treated with ice-cold water, and the obtained product is filtering and crystalizing from of yellow crystal, as in the Figure(3)

yellow colour, mp 212-214 ˚C, m/z: 279.2 ,FT-IR spectrum of compound shows the following bands: : stretched vibration band of group (NH_2) at (3355.52 cm-1),stretched vibration band of group (N-H) at (3149.74 cm-1) , stretched vibration band of group (C-H ar) at (3023.67 cm-1), stretched vibration band of group (C-H al) at (2884.21 cm-1), stretched vibration band of group (C=O keton) at (1718.02 cm-1), stretched vibration band of group (C=N) at (1681.84 cm-1) , stretched vibration band of group (C=C ar) at (1463.54-1585.54 cm-1), stretched vibration band of group (C-N aryl) at (1300.59 cm-1), and the stretched vibration band of group (O.O.P aryl) at (777.58-831.98 cm-1). 1H NMR (400 MHz, DMSO-d6) δ 10.22 (s,1H, NH), 7.30 (s, 1H, NH), 7.56 - 6.71 (m, 8H, Aromatic) 5.27 (s, 2H, NH2), 3.63 - 3.43 (m, 2H, -CH2-).13C NMR (100 MHz, DMSO-d6) δ 149.3, 148.1, 140.3, 129.0, 127.0, 124.8, 123.5, 123.3, 119.67, 114.2, 110.9, 68.5, 42.5.

Study of biological activities:

Antibacterial Activity Test

To evaluate the anti-bacterial growth efficacy of some prepared compounds, both Gram-positive and Gram-negative bacteria were selected. Standard procedures with commercially available Nutrient agar (Acumedia/LAB) were followed to prepare Nutrient agar plates. A total of 28 g of Nutrient agar was added to 1 L of distilled water in a conical flask. The mixture was stirred and heated until completely dissolved. The flask was stoppered with cotton, and the medium was sterilized in an autoclave for 20 minutes at 121°C under a pressure of 15 pounds per square inch. After sterilization, the medium was cooled to 45-55°C and poured into petri dishes, with approximately 15-20 mL per dish. The dishes were then allowed to cool and solidify, rendering the medium ready for bacterial growth.

The antibacterial compounds' effectiveness was assessed using four types of bacteria to investigate bacterial growth inhibition rates: Staphylococcus aureus and Streptococcus spp. (Gram-positive), and Pseudomonas aeruginosa and Escherichia coli (Gram-negative). The Kirby-Bauer method was employed for sensitivity testing. Four colonies of each bacterial type were transferred to the Nutrient agar medium and incubated at 37°C for 15-16 hours. A saline solution (Normal saline) was diluted, and 0.1 mL of the bacterial suspension was transferred to the Nutrient agar plates and spread evenly on the surface. The plates were left for approximately 30 minutes before further analysis.

To evaluate the inhibitory effects of the prepared chemical compounds, tablets were extracted from the filter flask and submerged in solutions of varying compound concentrations, which were then examined for antibacterial activity. These solutions were prepared using N,N-dimethylformamide as a solvent. The saturated tablets were evenly distributed across the agar surface at appropriate intervals and left to incubate for 20-24 hours.

Gentamycin and Tetracycline antibiotics were employed as references for bacterial inhibition, consistent with standard practices in public health laboratories and endorsed by WHO protocols, targeting the four specified bacterial species. The diameter of inhibition zones was measured, and each experiment was repeated thrice to ensure reliability. The results, including the examination of inhibition zones depicted in Figure 4 and the preliminary screening test outcomes listed in Table 1, were documented for analysis.

Antifungal Activity Test

The antifungal activity was estimated using the agar dilution method, with slight modifications, for determining the inhibition of mycelial radial growth of test organisms by the prepared compounds. Two types of fungi were pathologically tested and cultured on Potato-Dextrose-Agar (PDA) as per the manufacturer's instructions. PDA was prepared by dissolving 39 g in 1 L distilled water, sterilized by autoclaving for 20 minutes at 121°C and 15 lb/in^2 pressure, then cooled to 45°C in a water bath. After cooling, ampicillin antibiotic at 42 mg/L was added to prevent bacterial growth.

Prepared compounds were dissolved in N,N-dimethylformamide (DMF), and sterile filter papers were saturated with various concentrated solutions. In a laminar flow cabinet, the medium was poured into 90 mm sterile plastic Petri dishes at 40-45°C and allowed to set. Each test plate's center was inoculated with a 6 mm plug of 5-day-old cultures for each pathogen separately. A control plate containing only the 6 mm fungal plug in the basal medium was included.

The plates were then incubated for 5 days (Aspergillus niger) and 7 days (Candida albicans) in a growth cabinet at 25±2°C. Each assay was replicated twice, and the screening procedure was repeated twice. Radial mycelial growth was evaluated daily for 5 days (Aspergillus niger) and 7 days (Candida albicans) by calculating the mean of two perpendicular colony diameters for each replicate. The values were expressed in millimeters per day and calculated as percentage mycelial growth inhibition using the following formula:

$$\% \text{ mycelial growth inhibition} = \frac{G_{Control} - G_{Test}}{G_{Control}} * 100$$

Where:

$G_{Control}$ = Average diameter of the fungal colony of the control.

G_{Test} = Average diameter of the fungal colony treated with the prepared compounds.

The data from two screening experiments are pooled and averaged and then the inhibition zones that are caused by the various compounds are examined and shown in figures (5),(6), and the preliminary screening tests results are listed in table

Geometry optimization for the lead molecules:

The ideal geometric configuration and electronic properties of the prepared compounds were investigated using computational methods. Theoretical calculations were performed with the Gaussian 09W program, employing the 6-311G(d,p) basis set. Geometry optimization based on energy considerations was executed using the B3LYP density functional, incorporating Becke's gradient exchange correction, Parr correlation functional, and the Lee-Yang-Vosko/Wilk-Nusair correlation functional.

To begin the process, the Gaussian 09W program viewer was opened. The prepared spiroheterocyclic compound files (.mol) were loaded using the 'File Open' option. The Gaussian Calculation Setup was then accessed to configure the job type for optimization. The method selected was DFT with B3LYP and the 6-311G(d,p) basis set. The initial guess was set to mix HOMO and LUMO orbitals, and the job was submitted for calculation.

Upon completion of the calculation process, two files with different extensions (.chk and .log) were generated. These files were used to view the results of the calculations. To obtain and visualize the energy of the HOMO and LUMO orbitals and their forms, the following steps were taken: Tools → MOs → Select the required orbitals → Visualize → Update → OK.

Results and Discussion

Synthesis and Characterization of Compounds

A small library comprising four compounds (A1-A4) was synthesized using isatin and primary derivatives, with acetic acid (1 ml) employed as a refluxing agent for 2-9 hours. Subsequently, six final compounds (Z1-Z6) were produced utilizing mercaptoacetic acid and prepared Schiff bases, with dry dioxane serving as a solvent for Z1 and Z3, and benzene for Z4, in the presence of anhydrous zinc chloride.

Refluxing the reaction components in ethanol for 2-15 hours yielded moderate to good yields of both A1-A4 and Z1-Z6, which were isolated via simple filtration of directly precipitated products. The purity of these compounds, determined by FTIR spectrum analysis, ranged from approximately 90-98%. Following recrystallization, needle-like crystals were obtained, varying in color from yellow to orange.

The substituted spiroheterocyclic compounds were synthesized using mercaptoacetic acid and Schiff bases, employing dry dioxane

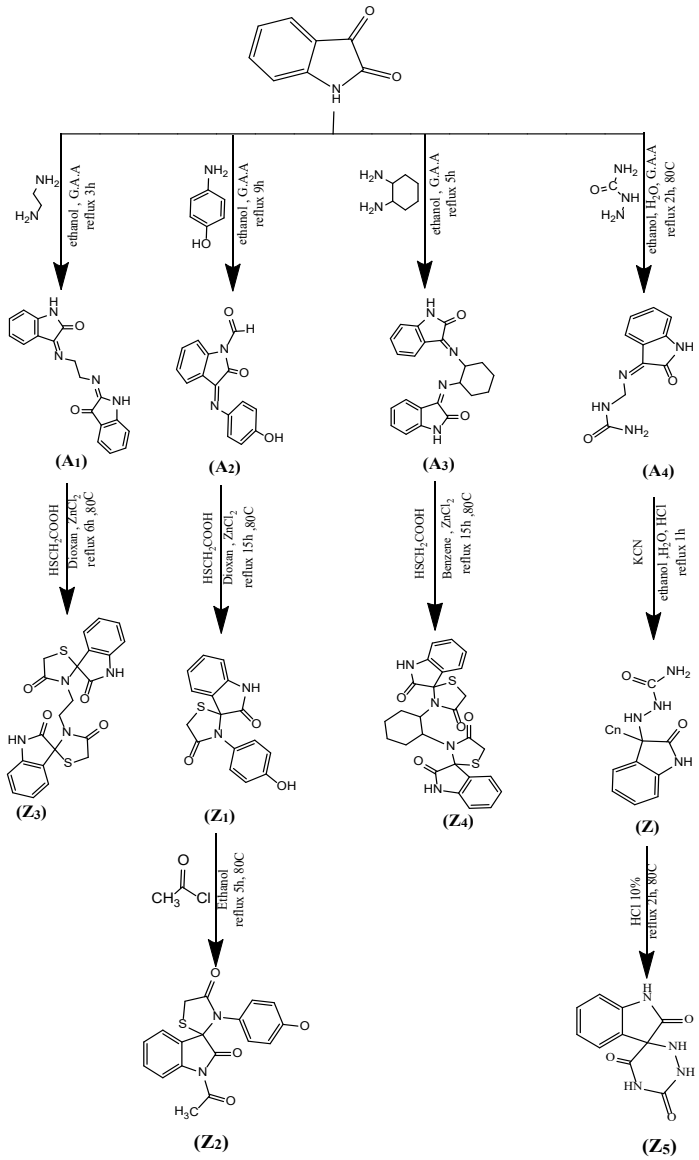

Figure 1. Synthesis spiroheteroctclic from isatin (Z_1-Z_6)

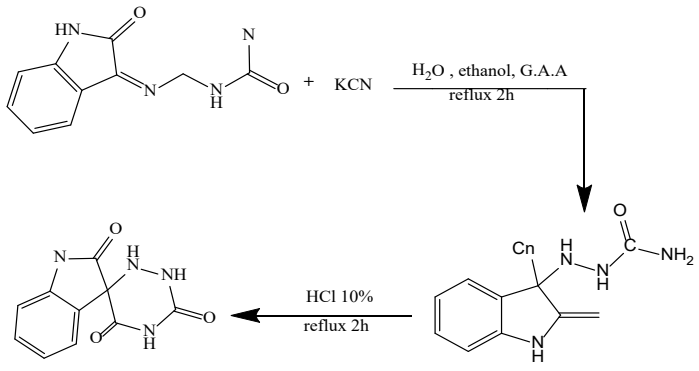

Figure 2. Indoline-3,6'-[1,2,4]triazinane]-2,3',5'-trione (Z_5)

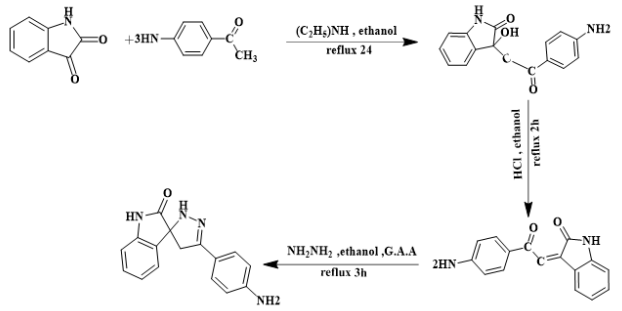

Figure 3. 5'-(4-aminophenyl)-2',4'-dihydrospiro[indoline-3,3'-pyrazol]-2-one (Z_6)

Table 1. Antibacterial activity data of the same prepared spiro compounds

	Gram-negative									
	Escherichia coli					***Pseudomonas aeruginosa***				
	Concentration (mg/mL)					**Concentration (mg/mL)**				
compound	1.25	2.5	5	12.5	25	1.25	2.5	5	12.5	25
Z_2	10	14	19	22	29	9	14	19	24	30
Z_3	*	*	*	18	22	*	*	9	15	20
Z_4	9	15	20	25	28	10	13	19	24	27
Z_5	11	14	19	24	29	10	13	20	26	31
Z_6	10	14	19	26	30	8	13	21	27	31
Gentamycin	7	12	20	27	31	12	14	20	28	30
Tetracycline	5	9	17	23	27	7	11	13	15	24
DMF	*	*	*	*	*	*	*	*	*	*

	Gram-positive									
	Staphylococcus aureus					***Streptococcus spp.***				
	Concentration (mg/mL)					**Concentration (mg/mL)**				
compound	1.25	2.5	5	12.5	25	1.25	2.5	5	12.5	25
Z_2	12	16	26	31	33	18	22	27	30	36
Z_3	*	7	11	19	23	*	*	9	14	19
Z_4	6	13	16	23	28	10	15	20	27	30
Z_5	10	17	30	35	38	11	20	27	29	33
Z_6	22	25	30	34	37	12	15	25	31	35
Gentamycin	10	15	27	36	39	13	14	29	31	34
Tetracycline	11	17	29	34	36	10	12	26	30	35
DMF	*	*	*	*	*	*	*	*	*	*

* No bacterial growth was observed.

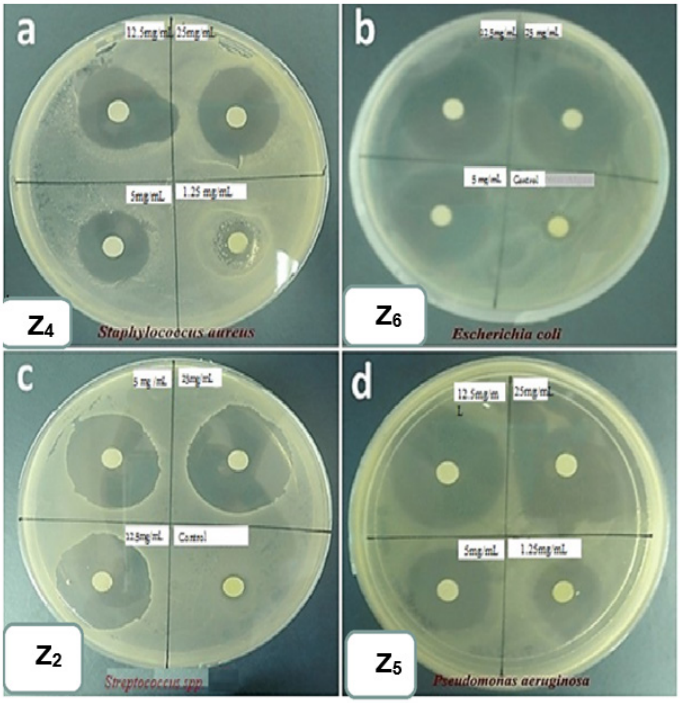

Figure (4): Antibacterial activity of prepared spiro compounds

Table 2. Percentage mycelial growth inhibition data of the prepared spiro compounds

	Candida albicans					**Aspergillus niger**				
	Concentration (mg/mL)					**Concentration (mg/mL)**				
Compound	1.25	2.5	5	12.5	25	1.25	2.5	5	12.5	25
Z2	*	25	36	43	47	11	22	34	49	55
Z3	15	27	39	47	58	*	*	20	53	67
Z4	*	20	28	35	40	10	20	33	48	50
Z5	9	22	35	43	56	11	17	34	41	43
Z6	8	20	30	45	58	10	23	40	46	47
Fluconazole	14	20	47	64	76	13	22	43	65	72
DMF	*	*	*	*	*	*	*	*	*	*

* No effect on the growth of the fungus was observed.

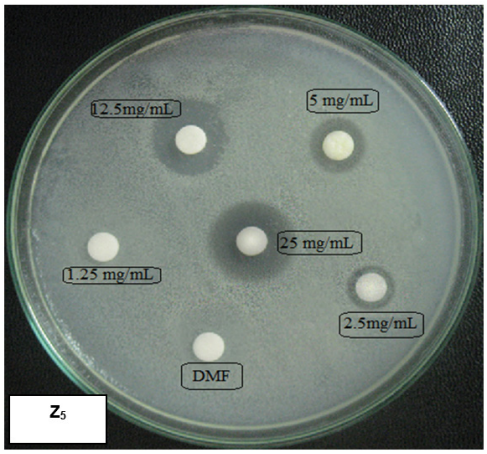

Figure 5. Anti-fungi activity of prepared spiro compounds against *Candida albicans*

for Z1 and Z3, and benzene for Z4 with anhydrous zinc chloride (ZnCl2). Compound Z2 was synthesized from Z1 by dissolving it in pyridine and adding acetyl chloride dropwise in an ice bath. The previously prepared Schiff base A4 was dissolved in a mixture of ethanol and glacial acetic acid (G.A.A) before further processing with KCN.

The procedure involved mixing the components and subjecting them to sublimation for two hours. After forming a precipitate by adding 10 ml of 10% HCl, the mixture underwent reflux for another two hours (Z5). Isatin was dissolved in ethanol, with the addition of 5 drops of G.A.A. 4-amino acetophenone, also dissolved in ethanol, was combined with the previous mixture. Sublimation was performed for 24 hours, followed by dissolution in ethanol and the addition of 1 ml of concentrated HCl. The mixture was heated for two hours, cooled, and added to ice. Another mixture was prepared with hydrazine hydrate dissolved in ethanol and acetic acid, and refluxed for 3 hours to yield Z6.

Schiff bases and mercaptoacetic acid were reacted in refluxing ethanol to produce the desired compounds. TLC monitored the reaction progress. After cooling, the condensate was filtered and purified via recrystallization from ethanol. Structural determination and signal assignments of the final products (Z1-Z6) were accomplished using FTIR, NMR, and other spectroscopic techniques. The physical properties of some synthesized derivatives were also documented.

Structural and Computational Analysis

The structure of the synthesized systems was determined through melting point analysis and spectroscopic data obtained from 1H NMR, FT-IR, mass, and 13C NMR techniques. Computational methods were utilized to explore optimized geometric boundaries such as bond angles and lengths, as well as the ground state electronic properties of the hetero spiro cyclic compounds.

Theoretical calculations for the prepared spiroheterocyclic compounds were conducted using the Gaussian 09W program package. Density functional theory (DFT) at the B3LYP level and the 6-311G(d,p) basis set approximation method were employed. DFT enabled the investigation of the relationship between geometry and electronic properties, such as the calculation of HOMO and LUMO energies. The localization of the HOMO orbital indicated the nucleophilic site's electron density, influencing ionization potential effects, while the localization of the LUMO predicted good electrophilic sites, correlating to electron affinity.

Supp. Tables (1 - 8) present the calculated HOMO and LUMO energies along with bond angles and lengths. Molecular parameters such as bond angles, bond lengths, ELUMO, EHOMO, and the energy gap (Egap = ELUMO - EHOMO) were examined using DFT and B3LYP methods with 6-311G(d,p) basis sets, as summarized in Supp. Table (8). The Egap value, reflecting the energy difference between LUMO and HOMO, is crucial in assessing molecular stability and reactivity. Lower Egap values indicate higher chemical reactivity but lower stability.

Supp. Table (10) further elaborates on properties derived from HOMO and LUMO parameters, including ionization potential (IE), electron affinity (EA), electronegativity (χ), resistance (η), electronic chemical potentials (Pi), absolute softness (σ), electron accepting tendency (ω), and overall molecular properties (Ƨ). Additionally, ΔNmax, indicating the fraction of electrons transferred in a chemical reaction, can be determined using electronegativity and global hardness values obtained through DFT calculations.

Biological Activity of Prepared Compounds

The antibacterial and antifungal activity of several prepared compounds were fully assessed. This evaluation involved measuring the inhibition zones, represented by the bacteria-free area surrounding the discs. The results of these tests are comprehensively presented and elucidated in Tables 1 and 2, as well as Figures 4, 5, and 6. Varied inhibitory diameters were observed across the compounds, influenced by factors such as compound nature, ring type, material concentration, and the specific bacteria strains under examination.

Antibacterial Activity

The results indicated that the compound 2'-(4-aminobenzoyl)-1-((diethylamino)methyl)-1'-(4-nitrophenyl)-1',2',5',6',7',7a'-hexahydrospiro[indoline-3,3'-pyrrolizin]-2-one was inhibitory to Escherichia coli at a concentration of 25 mg/ml, showing the least inhibitory strength at 1.25 mg/ml. This compound showed the highest inhibitory power against Pseudomonas aeruginosa at a concentration of 25 mg/ml.

Compound 1'-(4-bromobenzoyl)-2'-phenyl-1',2',5',6',7',7a'-hexahydrospiro[indene-2,3'-pyrrolizin]-1,3-dione showed the highest inhibitory power against both Escherichia coli and Pseudomonas aeruginosa at a concentration of 25 mg/ml. Similarly, spiro[indoline-3,6'-[1,2,4]triazinane]-2,3',5'-trione exhibited the highest inhibitory power against Escherichia coli and Pseudomonas aeruginosa at a concentration of 25 mg/ml.

Other compounds, including 2'-(4-aminobenzoyl)-1'-(4-nitrophenyl)-1',2',5',6',7',7a'-hexahydrospiro[indoline-3,3'-pyrrolizin]-2-one, 3',3'''-(ethane-1,2-diyl)bis(spiro[indoline-3,2'-thiazolidine]-2,4'-dione), 3',3'''-(cyclohexane-1,2-diyl)bis(spiro[indoline-3,2'-thiazolidine]-2,4'-dione), 3'-(3-aminobenzoyl)-4'-(4-chlorophenyl)spiro[indoline-3,2'-pyrrolidin]-2-one, 1-acetyl-3'-(4-hydroxyphenyl)spiro[indoline-3,2'-thiazolidine]-2,4'-dione, 5'-(4-aminophenyl)-2',4'-dihydrospiro[indoline-3,3'-pyrazol]-2-one, 2'-(4-bromobenzoyl)-1'-phenyl-1',2',5',6',7',7a'-hexahydrospiro[indoline-3,3'-pyrrolizin]-2-one, and 7-amino-2',4-dioxo-2-thioxo-2,3,4,4a-tetrahydrospiro[cyclopenta[d]pyrimidine-5,3'-indoline]-6-

carbonitril, showed strong inhibition of both Escherichia coli and Pseudomonas aeruginosa at 25 mg/ml.

The antibiotic gentamicin exhibited the highest inhibitory power for both types of bacteria, with results reaching 31 mm at a concentration of 25 mg/ml for Escherichia coli, while it showed an inhibitory power of 30 mm at 25 mg/ml for Pseudomonas aeruginosa.

Antifungal Activity

Compound 2'-(4-aminobenzoyl)-1-((diethylamino)methyl)-1'-(4-nitrophenyl)-1',2',5',6',7',7a'-hexahydrospiro[indoline-3,3'-pyrrolizin]-2-one exhibited inhibitory effects on Candida albicans at 25 mg/ml, with the least inhibition observed at 1.25 mg/ml. It displayed the highest inhibitory potency against Aspergillus niger at 25 mg/ml. Compound 1'-(4-bromobenzoyl)-2'-phenyl-1',2',5',6',7',7a'-hexahydrospiro[indene-2,3'-pyrrolizine]-1,3-dione demonstrated maximum inhibition against both Candida albicans and Aspergillus niger at 25 mg/ml.

Spiro[indoline-3,6'-[1,2,4]triazinane]-2,3',5'-trione also exhibited the highest inhibitory strength against both Candida albicans and Aspergillus niger at 25 mg/ml. Other compounds displayed strong inhibition against both fungi types at a concentration of 25 mg/ml. Gentamycin showed the highest inhibitory potency against both fungi types, with an inhibitory power of 31 mm for Candida albicans and 30 mm for Aspergillus niger at a concentration of 25 mg/ml.

Conclusion

In conclusion, the synthesized compounds exhibited promising biological activities against various bacterial and fungal strains, with some compounds demonstrating significant inhibitory effects. The theoretical and computational analysis provided valuable insights into the electronic properties and stability of the synthesized molecules, contributing to a better understanding of their reactivity and potential applications. These findings underscore the importance of continued research and development in the field of spiroheterocyclic compounds for potential therapeutic applications.

Author contributions

Z.A.A.H., A.K.A.N. conceptualized, analyzed data, edited and reviewed the manuscript. All authors read and approved the final version of the manuscript.

Acknowledgment

The authors thanked the Department.

Competing financial interests

The authors have no conflict of interest.

References

Abdella, A. M., Abdelmoniem, A. M., Abdelhamid, I. A., & Elwahy, A. H. M. (2020). Synthesis of heterocyclic compounds via Michael and Hantzsch reactions. Journal of Heterocyclic Chemistry, 57(4), 1476–1523. doi:10.1002/jhet.3883.

Abdella, A. M., Abdelmoniem, A. M., Abdelhamid, I. A., & Elwahy, A. H. M. (2020). Synthesis of heterocyclic compounds via Michael and Hantzsch reactions. Journal of Heterocyclic Chemistry, 57(4), 1476–1523. https://doi.org/10.1002/jhet.3883

Adlu, M., & Yavari, I. (2023). One-pot, mild and efficient multicomponent synthesis of novel various spiro-nitrogen heterocycle compounds. Bull. Chem. Soc. Ethiop., 37(1), 115–122.

Adlu, M., & Yavari, I. (2023). One-pot, mild and efficient multicomponent synthesis of novel various spiro-nitrogen heterocycle compounds. Bull. Chem. Soc. Ethiop., 37(1), 115–122.

Adlu, M., & Yavari, I. (2023). One-pot, mild and efficient multicomponent synthesis of novel various spiro-nitrogen heterocycle compounds. Bulletin of the Chemical Society of Ethiopia, 37(1), 115–122.

Al-Naseeri, A. K. A., Saleh, H. K., & Jassim, I. K. (2021). Synthesis, characterization, and theoretical study of new schiff bases from (S)-2-amino-3-(3,4-dihydroxyphenyl)-2-methyl propanoic acid as initial material of 1,3-oxazepine-1,5-dione. Int. J. Drug Deliv. Technol., 11(2), 258–264. doi:10.25258/ijddt.11.2.3.

Al-Naseeri, A. K. A., Saleh, H. K., & Jassim, I. K. (2021). Synthesis, characterization, and theoretical study of new schiff bases from (S)-2-amino-3-(3,4-dihydroxyphenyl)-2-methyl propanoic acid as initial material of 1,3-oxazepine-1,5-dione. International Journal of Drug Delivery Technology, 11(2), 258–264. https://doi.org/10.25258/ijddt.11.2.3

Aytac, S., Gundogdu, O., Bingol, Z., & Gulcin, İ. (2023). Synthesis of Schiff Bases Containing Phenol Rings and Investigation of Their Antioxidant Capacity, Anticholinesterase, Butyrylcholinesterase, and Carbonic Anhydrase Inhibition Properties. Pharmaceutics, 15(3), 779. doi:10.3390/pharmaceutics15030779.

Aytac, S., Gundogdu, O., Bingol, Z., & Gulcin, İ. (2023). Synthesis of Schiff Bases Containing Phenol Rings and Investigation of Their Antioxidant Capacity, Anticholinesterase, Butyrylcholinesterase, and Carbonic Anhydrase Inhibition Properties. Pharmaceutics, 15(3), 779. https://doi.org/10.3390/pharmaceutics15030779

Bashar, B. S., et al. (2022). Application of novel Fe3O4/Zn-metal organic framework magnetic nanostructures as an antimicrobial agent and magnetic nanocatalyst in the synthesis of heterocyclic compounds. Front. Chem., 10, 1–17. doi:10.3389/fchem.2022.1014731.

Bashar, B. S., et al. (2022). Application of novel Fe3O4/Zn-metal organic framework magnetic nanostructures as an antimicrobial agent and magnetic nanocatalyst in the synthesis of heterocyclic compounds. Frontiers in Chemistry, 10. https://doi.org/10.3389/fchem.2022.1014731

Brandl, M. T. (2006). Fitness of human enteric pathogens on plants and implications for food safety. Annu. Rev. Phytopathol., 44, 367–392. doi:10.1146/annurev.phyto.44.070505.143359.

Brandl, M. T. (2006). Fitness of human enteric pathogens on plants and implications for food safety. Annual Review of Phytopathology, 44, 367–392. https://doi.org/10.1146/annurev.phyto.44.070505.143359

Canneaux, S., Bohr, F., & Henon, E. (2014). KiSThelP: a program to predict thermodynamic properties and rate constants from quantum chemistry results. J. Comput. Chem., 35(1), 82–93.

Canneaux, S., Bohr, F., & Henon, E. (2014). KiSThelP: A program to predict thermodynamic properties and rate constants from quantum chemistry results. Journal of Computational Chemistry, 35(1), 82–93.

Dabhi, R. A., Dhaduk, M. P., Bhatt, V. D., & Bhatt, B. S. (2022). Synthetic approach toward spiro quinoxaline-β-lactam based heterocyclic compounds: Spectral characterization, SAR, pharmacokinetic and biomolecular interaction studies. Journal of Biomolecular Structure and Dynamics. doi: 10.1080/07391102.2022.2086176.

Dabhi, R. A., Dhaduk, M. P., Bhatt, V. D., & Bhatt, B. S. (2022). Synthetic approach toward spiro quinoxaline-β-lactam based heterocyclic compounds: Spectral characterization, SAR, pharmacokinetic and biomolecular interaction studies. Journal of Biomolecular Structure and Dynamics. doi:10.1080/07391102.2022.2086176

Dabhi, R. A., Dhaduk, M. P., Bhatt, V. D., & Bhatt, B. S. (2022). Synthetic approach toward spiro quinoxaline-β-lactam based heterocyclic compounds: Spectral characterization, SAR, pharmacokinetic and biomolecular interaction studies. Journal of Biomolecular Structure and Dynamics. https://doi.org/10.1080/07391102.2022.2086176

Izsák, R., et al. (2023). Quantum computing in pharma: A multilayer embedding approach for near future applications. J. Comput. Chem., 44(3), 406–421.

Izsák, R., et al. (2023). Quantum computing in pharma: A multilayer embedding approach for near future applications. J. Comput. Chem., 44(3), 406–421.

Izsák, R., et al. (2023). Quantum computing in pharma: A multilayer embedding approach for near future applications. Journal of Computational Chemistry, 44(3), 406–421.

Kareem, A., & Humadi, A. (2009). The cemecales.

Kareem, A., & Humadi, A. (2009). The cemecales.

Kareem, A., & Humadi, A. (2009). The cemecales.

Kumar, T., Satam, N., & Namboothiri, I. N. N. (2016). Hauser–Kraus Annulation of Phthalides with Nitroalkenes for the Synthesis of Fused and Spiro Heterocycles. European J. Org. Chem., 2016(20), 3316–3321.

Kumar, T., Satam, N., & Namboothiri, I. N. N. (2016). Hauser–Kraus Annulation of Phthalides with Nitroalkenes for the Synthesis of Fused and Spiro Heterocycles. European J. Org. Chem., 2016(20), 3316–3321.

Kumar, T., Satam, N., & Namboothiri, I. N. N. (2016). Hauser–Kraus Annulation of Phthalides with Nitroalkenes for the Synthesis of Fused and Spiro Heterocycles. European Journal of Organic Chemistry, 2016(20), 3316–3321.

Lamont, R. J., Hajishengallis, G. N., & Jenkinson, H. F. (2014). Oral microbiology and immunology. (2nd ed.). ASM press.

Lamont, R. J., Hajishengallis, G. N., & Jenkinson, H. F. (2014). Oral microbiology and immunology (2nd ed.). ASM Press.

Lopes Lima, K. A., & Ribeiro, L. A. (2023). A DFT study on the mechanical, electronic, thermodynamic, and optical properties of GaN and AlN counterparts of biphenylene network. Mater. Today Commun., 37, 1–22. doi: 10.1016/j.mtcomm.2023.107183.

Lopes Lima, K. A., & Ribeiro, L. A. (2023). A DFT study on the mechanical, electronic, thermodynamic, and optical properties of GaN and AlN counterparts of biphenylene network. Mater. Today Commun., 37, 1–22. doi:10.1016/j.mtcomm.2023.107183.

Lopes Lima, K. A., & Ribeiro, L. A. (2023). A DFT study on the mechanical, electronic, thermodynamic, and optical properties of GaN and AlN counterparts of biphenylene network. Materials Today Communications, 37, 1–22. https://doi.org/10.1016/j.mtcomm.2023.107183

Marsh, P. D., Lewis, M. A. O., Williams, D. W., & Martin, M. V. (2009). Oral microbiology E-book. Elsevier health sciences.

Marsh, P. D., Lewis, M. A. O., Williams, D. W., & Martin, M. V. (2009). Oral microbiology E-book. Elsevier Health Sciences.

Martínez, J., et al. (2023). Computational Studies of Aflatoxin B1 (AFB1): A Review. Toxins (Basel), 15(2). doi: 10.3390/toxins15020135.

Martínez, J., et al. (2023). Computational Studies of Aflatoxin B1 (AFB1): A Review. Toxins (Basel)., 15(2). doi:10.3390/toxins15020135.

Martínez, J., et al. (2023). Computational Studies of Aflatoxin B1 (AFB1): A Review. Toxins (Basel), 15(2). https://doi.org/10.3390/toxins15020135

Pederson, R., Kalita, B., & Burke, K. (2022). Machine learning and density functional theory. Nat. Rev. Phys., 4(6), 357–358.

Pederson, R., Kalita, B., & Burke, K. (2022). Machine learning and density functional theory. Nat. Rev. Phys., 4(6), 357–358.

Pederson, R., Kalita, B., & Burke, K. (2022). Machine learning and density functional theory. Nature Reviews Physics, 4(6), 357–358.

Raju, R., Raghunathan, R., Arumugam, N., Almansour, A. I., & Kumar, R. S. (2020). Regio- and stereoselective synthesis of novel β-lactam engrafted spiroheterocyclic hybrids via one-pot three component cycloaddition strategy. Tetrahedron Lett., 61(52), 152661.

Raju, R., Raghunathan, R., Arumugam, N., Almansour, A. I., & Kumar, R. S. (2020). Regio- and stereoselective synthesis of novel β-lactam engrafted spiroheterocyclic hybrids via one-pot three component cycloaddition strategy. Tetrahedron Letters, 61(52), 152661.

Singh, G. S., & Desta, Z. Y. (2012). Isatins as privileged molecules in design and synthesis of spiro-fused cyclic frameworks. Chem. Rev., 112(11), 6104–6155. doi: 10.1021/cr300135y.

Singh, G. S., & Desta, Z. Y. (2012). Isatins as privileged molecules in design and synthesis of spiro-fused cyclic frameworks. Chem. Rev., 112(11), 6104–6155. doi:10.1021/cr300135y.

Singh, G. S., & Desta, Z. Y. (2012). Isatins as privileged molecules in design and synthesis of spiro-fused cyclic frameworks. Chemical Reviews, 112(11), 6104–6155. https://doi.org/10.1021/cr300135y

Villarreal, Y., Insuasty, B., Abonia, R., Ortiz, A., Romo, P., & Quiroga, J. (2021). Three-component one-pot synthesis of new spiro[indoline-pyrrolidine] derivatives mediated by 1,3-dipolar reaction and DFT analysis. Monatshefte fur Chemie, 152(5), 497–506. doi:10.1007/s00706-021-02765-z.

Villarreal, Y., Insuasty, B., Abonia, R., Ortiz, A., Romo, P., & Quiroga, J. (2021). Three-component one-pot synthesis of new spiro[indoline-pyrrolidine] derivatives mediated by 1,3-dipolar reaction and DFT analysis. Monatshefte fur Chemie, 152(5), 497–506. https://doi.org/10.1007/s00706-021-02765-z

Yang, L., Liu, Y., Sternberg, C., & Molin, S. (2010). Evaluation of enoyl-acyl carrier protein reductase inhibitors as Pseudomonas aeruginosa quorum-quenching reagents. Molecules, 15(2), 780–792. doi:10.3390/molecules15020780.

Yang, L., Liu, Y., Sternberg, C., & Molin, S. (2010). Evaluation of enoyl-acyl carrier protein reductase inhibitors as Pseudomonas aeruginosa quorum-quenching reagents. Molecules, 15(2), 780–792. https://doi.org/10.3390/molecules15020780

Yuan, Y., et al. (2020). Synthesis of Spiro[5.n (n=6–8)]heterocycles through Successive Ring-Expansion/Indole C-2 Functionalization. Adv. Synth. Catal., 362(6), 1298–1302. doi: 10.1002/adsc.201901631.

Yuan, Y., et al. (2020). Synthesis of Spiro[5.n (n=6–8)]heterocycles through Successive Ring-Expansion/Indole C-2 Functionalization. Adv. Synth. Catal., 362(6), 1298–1302. doi:10.1002/adsc.201901631.

Yuan, Y., et al. (2020). Synthesis of Spiro[5.n (n=6–8)]heterocycles through Successive Ring-Expansion/Indole C-2 Functionalization. Advanced Synthesis & Catalysis, 362(6), 1298–1302